



**Calhoun: The NPS Institutional Archive**  
**DSpace Repository**

---

Theses and Dissertations

1. Thesis and Dissertation Collection, all items

---

1988

Development of a boundary layer control  
device for tip clearance experiments in an  
axial compressor

Tarigan, Muliukur.

Monterey, California : Naval Postgraduate School

---

<http://hdl.handle.net/10945/23016>

---

*Downloaded from NPS Archive: Calhoun*



Calhoun is the Naval Postgraduate School's public access digital repository for research materials and institutional publications created by the NPS community. Calhoun is named for Professor of Mathematics Guy K. Calhoun, NPS's first appointed -- and published -- scholarly author.

**Dudley Knox Library / Naval Postgraduate School**  
**411 Dyer Road / 1 University Circle**  
**Monterey, California USA 93943**

<http://www.nps.edu/library>



FIDELITY NATIONAL BANK  
EL PASO, TEXAS  
MONTEREY, CALIFORNIA 95034-3002





# NAVAL POSTGRADUATE SCHOOL

## Monterey, California



# THESIS

T13935

DEVELOPMENT OF A BOUNDARY LAYER  
CONTROL DEVICE FOR TIP CLEARANCE EXPERIMENTS  
IN AN AXIAL COMPRESSOR

by

Muliukur Tarigan

March 1988

Thesis Advisor:

R. P. Shreeve

Approved for public release; distribution is unlimited.

T239283



## REPORT DOCUMENTATION PAGE

1a REPORT SECURITY CLASSIFICATION <b>UNCLASSIFIED</b>			1b RESTRICTIVE MARKINGS		
2a SECURITY CLASSIFICATION AUTHORITY			3 DISTRIBUTION / AVAILABILITY OF REPORT Approved for public release; distribution is unlimited.		
2b DECLASSIFICATION/DOWNGRADING SCHEDULE					
4 PERFORMING ORGANIZATION REPORT NUMBER(S)			5 MONITORING ORGANIZATION REPORT NUMBER(S)		
6a NAME OF PERFORMING ORGANIZATION Naval Postgraduate School		6b OFFICE SYMBOL (if applicable) 67	7a NAME OF MONITORING ORGANIZATION Naval Postgraduate School		
6c ADDRESS (City, State, and ZIP Code) Monterey, California 93943-5000			7b ADDRESS (City, State, and ZIP Code) Monterey, California 93943-5000		
8a NAME OF FUNDING SPONSORING ORGANIZATION		8b OFFICE SYMBOL (if applicable)	9 PROCUREMENT INSTRUMENT IDENTIFICATION NUMBER		
8c ADDRESS (City, State, and ZIP Code)			10 SOURCE OF FUNDING NUMBERS		
			PROGRAM ELEMENT NO	PROJECT NO	TASK NO
			WORK UNIT ACCESSION NO		
11 TITLE (Include Security Classification) DEVELOPMENT OF A BOUNDARY LAYER CONTROL DEVICE FOR TIP CLEARANCE EXPERIMENTS IN AN AXIAL COMPRESSOR.					
12 PERSONAL AUTHOR(S) TARIGAN, MULIUKUR					
13a TYPE OF REPORT Master's Thesis		13b TIME COVERED FROM TO		14 DATE OF REPORT (Year, Month, Day) MARCH 1988	15 PAGE COUNT 66
16 SUPPLEMENTARY NOTES The views expressed in this thesis are those of the author and do not reflect the official policy or position of the Department of Defense or the United States Government.					
17 COSAT CODES			18 SUBJECT TERMS (Continue on reverse if necessary and identify by block number)		
FIELD	GROUP	SUB-GROUP	Boundary Layer Spires, Axial Compressor, Case-Wall Boundary Layer Control		
19 ABSTRACT (Continue on reverse if necessary and identify by block number) A boundary layer control device was designed to change significantly the case-wall boundary layer thickness entering a large-scale, multistage axial compressor. The device was intended to double the boundary layer thickness in order to evaluate the influence of the inlet boundary layer in controlled tip clearance experiments being conducted on the compressor. The boundary layer characteristics expected to be produced by the control device were predicted empirically and experimental verification was required. Kiel, cobra, and impact probes were used in the experiments and pressures were recorded manually using water manometers. The geometry of the boundary layer control device, an annular array of spires, was derived from shapes developed for simulating the atmospheric boundary layer in large rectangular section wind tunnels. A significantly thicker boundary layer was measured in the compressor than was intended. However, the results were interpreted and recommendations were made for geometry changes necessary to achieve the intended control for the tip clearance investigation.					
20 DISTRIBUTION / AVAILABILITY OF ABSTRACT <input checked="" type="checkbox"/> UNCLASSIFIED/UNLIMITED <input type="checkbox"/> SAME AS RPT <input type="checkbox"/> DTIC USERS			21 ABSTRACT SECURITY CLASSIFICATION <b>UNCLASSIFIED</b>		
22a NAME OF RESPONSIBLE INDIVIDUAL R.P. SHREEVE			22b TELEPHONE (Include Area Code) 408/646-2593		22c OFFICE SYMBOL 67Sf



Approved for Public Release; distribution is unlimited

Development of a Boundary Layer Control Device  
for Tip Clearance Experiments in an Axial Compressor

by

Muliukur Tarigan  
Major, Indonesian Air Force  
B.S., Indonesian Air Force Academy, 1966

Submitted in partial fulfillment of the  
requirements for the degree of

MASTER OF SCIENCE IN AERONAUTICAL ENGINEERING

from the

NAVAL POSTGRADUATE SCHOOL  
March 1988

## ABSTRACT

A boundary layer control device was designed to change significantly the case-wall boundary layer thickness entering a large-scale, multistage axial compressor. The device was intended to double the boundary layer thickness in order to evaluate the influence of the inlet boundary layer in controlled tip clearance experiments being conducted on the compressor. The boundary layer characteristics expected to be produced by the control device were predicted empirically and experimental verification was required. Kiel, cobra, and impact probes were used in the experiments and pressures were recorded manually using water manometers. The geometry of the boundary layer control device, an annular array of spires, was derived from shapes developed for simulating the atmospheric boundary layer in large rectangular section wind tunnels. A significantly thicker boundary layer was measured in the compressor than was intended. However, the results were interpreted and recommendations were made for geometry changes necessary to achieve the intended control for the tip clearance investigation.

## TABLE OF CONTENTS

I.	INTRODUCTION .....	1
II.	COMPRESSOR AND OPERATION .....	4
	A. COMPRESSOR .....	4
	B. INSTRUMENTATION and DATA COLLECTION .....	14
III.	BOUNDARY LAYER CONTROL DEVICE .....	21
	A. DESIGN INTENT .....	21
	1. Requirements & Approach .....	21
	2. Design .....	22
	B. CONSTRUCTION .....	26
IV.	TEST PROGRAM .....	28
	A. PRELIMINARY TEST .....	28
	B. STATIC PRESSURE DISTRIBUTION MEASUREMENTS .....	31
	C. BOUNDARY LAYER MEASUREMENTS .....	31
V.	ANALYSIS AND DISCUSSION .....	36
	A. CALCULATION OF DISPLACEMENT THICKNESS .....	36
	B. COMPARISON WITH DESIGN INTENT .....	39
	1. Boundary Layer Thickness .....	39
	2. Profile Shape .....	47
	3. Other Considerations .....	47
	C. ACHIEVING THE REQUIRED CONTROL .....	48
VI.	CONCLUSIONS AND RECOMMENDATIONS .....	50
	LIST OF REFERENCES .....	52
	BIBLIOGRAPHY .....	53
	INITIAL DISTRIBUTION LIST .....	54

LIST OF TABLES

I.	Dimensions of Standard Half-Width Spires -----	24
II.	Throttle Element Arrangements-----	29
III.	Test Program Summary -----	30
IV.	Pressure Distribution Data for Configuration 1 -----	33
V.	Pressure Distribution Data for Configuration 2 -----	34
VI.	Integrated Velocity Profile Parameters for Configuration 1 -----	40
VII.	Integrated Velocity Profile Parameters for Configuration 2 -----	41

## LIST OF FIGURES

1. Compressor Test Rig -----	5
2. View of the Inlet Bellmouth Without (a) and With (b) a Protective Mesh Screen -----	6
3. Compressor Blading	
a. Flow Path View -----	7
b. Stage Tip Section -----	8
4. Velocity Diagram -----	10
5. View of the Compressor Test Rig -----	11
6. Electric Motor Drive -----	12
7. Throttle Showing Removable Elements -----	13
8. Arrangement of the Instrumentation -----	15
9. Probes	
a. Probe Tip Geometries -----	16
b. Views of Probe Tips and Actuators -----	17
10. Meriam Water Micromanometers	
a. Connections to the Probes -----	19
b. View of the Instruments -----	20
11. Compressor Throttle Section	
a. Element Positions -----	23
b. Spire and Plate Elements -----	23
12. Spire Element	
a. Circular Arrangement as Built -----	25
b. Linear Arrangement as Designed -----	25

13.	Spire Geometry	
a.	As Designed -----	27
b.	As Built -----	27
14.	Static Pressure Distribution Ahead of the IGV's at $P_{t_{CL}} - P_{sw} = 7.25$ Inches of Water -----	32
15.	Boundary Layer Profiles with Screens (Configuration 1) and Spires (Configuration 2) -----	35
16.	Determination of the Displacement Thickness For Configuration 1 -----	42
17.	Determination of the Displacement Thickness For Configuration 2 -----	43
18.	Comparison of Boundary Layers With and Without Spires -----	44
19.	Streamline Location for Uniform Inviscid Flow -----	45

# LIST OF SYMBOLS

$\rho$	- Density
$C_L$	- Center line
$P_{S_i}$	- Static pressure
$P_{S_w}$	- Static pressure at the case-wall
$P_t$	- Total pressure
$P_{t_{C_L}}$	- Total pressure at the center line
$R$	- Radius of the pipe
$r$	- Local radial displacement
$D$	- Diameter
$V$	- Velocity
$V_1$	- Absolute velocity into the rotor blade
$V_2$	- Absolute velocity out of the rotor blade
$V_\infty$	- Reference velocity derived from measurements (Eq.(2))
$V_{C_L}$	- Velocity at the center line
$V_i$	- Local velocity
$W_1$	- Relative velocity into the rotor
$W_2$	- Relative velocity out of the rotor
$U$	- Wheel speed
$s$	- Spire height
$h$	- Compressor annulus height
$\Delta$	- Displacement of uniform-flow, inviscid streamline passing through the spire tip, from the case-wall at the compressor inlet

LIST OF SYMBOLS (continued)

- $\delta$  - Boundary layer thickness
- $\delta^*$  - Boundary layer displacement thickness
- $t$  - Tip clearance
- $A$  - Area
- $V$  - Value of  $V/V_\infty$  at the edge of the boundary layer
- $y$  - Radial displacement inwards from the case-wall
- $\beta_1$  - Rotor inlet relative airflow angle with respect to the axis
- $\beta_2$  - Rotor outlet relative airflow angle with respect to the axis
- $\alpha_1$  - Rotor inlet absolute airflow angle with respect to the axis
- $\alpha_2$  - Rotor outlet absolute airflow angle with respect to the axis



## ACKNOWLEDGMENT

The author would like to thank the following people:

1. Professor R. P. Shreeve, Director of the Turbopropulsion Laboratory, Naval Postgraduate School, Monterey, California and his staff, Ian Moyle and Thaddeus Rest, for their guidance in this project. Without their assistance and the benefit of their experience, I could not have completed this thesis.
2. The NPS Photo Division for their effort and cooperation on the photographs required for my thesis.
3. My wife, Enny Sitepu; my sons, Suranta and Ferianta; and my daughters, Mena and Sabarina, who always supported my spirit during my studies.

## I. INTRODUCTION

Axial compressors in aircraft engines are generally designed for nearly uniform inlet flow conditions, with thin boundary layers, but are required to operate stably over a range of inlet flow distortion. It is found in practice that multi-stage core compressors, once developed, are then very sensitive to any change in the tip-gap between the rotor blades and the case-wall. In particular, changes in the tip-gap result in a reduction in the compressor efficiency and a loss of stability margin in distorted inflow. In view of the need to develop military aircraft engines with improved thrust-to-weight ratio and increased tolerance to distortion, attention has been given in recent years to understanding the effects of tip clearance change on the flow in axial compressors. A large scale, multistage axial compressor facility, which would allow experimental investigations to be made under well-controlled test conditions, was installed and prepared for that purpose. (Ref. 1)

The first experiment to be conducted in the facility is one in which the tip clearance will be increased systematically and data will be obtained from instrumentation designed to resolve the important changes in the internal flow field. However, the results of this experiment would be limited to the particular compressor-face inlet flow

conditions which the test installation generated. Unknown, a priori, is the importance of the inlet case-wall boundary layer profile, and thickness, in relation to the physical gap between the rotor and the case-wall. Thus, it is equally important to change the boundary layer as to change the clearance gap. The purpose of the present study was to develop an experimental technique to be used to control the boundary layer thickness entering the compressor.

The approach was to use an array of "spires" installed as a removable element in a throttle housing in the inlet duct. The presence, and design of the throttle, and the difficulty of alternate approaches such as providing suction on the scale required, suggested this solution. In the work that is reported here, the design of the spires is reviewed and a program of measurements to evaluate the effect of the spires on the compressor inlet case-wall boundary layer, is reported. The measurements showed that the boundary layer with the spires was thicker than was intended, and that the velocity profile was unacceptably distorted.

It was concluded that compromises which were made in the manufacture of the spires, which involved approximating the slender cusped shapes with linear cuts, were unacceptable. Also, the installation of the spires as a circular array within a round duct was quite different from the linear geometry within a large wind tunnel that had provided the data on which the design was based. Recommendations were

made for changes to be made to the spires to achieve the goal of doubling the inlet boundary layer thickness without changing the shape of the velocity profile.

## II. COMPRESSOR AND OPERATION

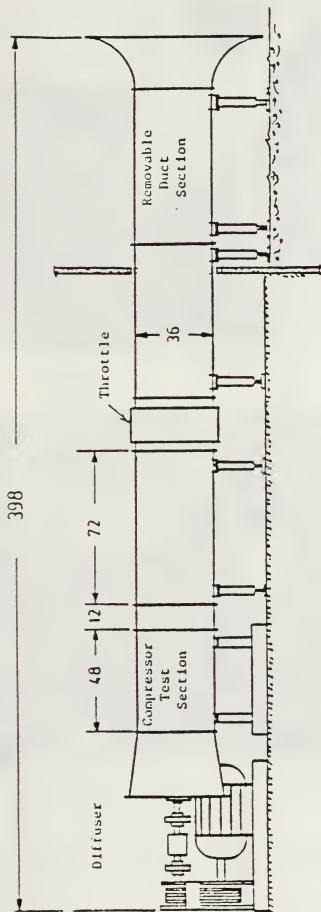
The compressor test facility, data collection method, and details of the instrumentation used are discussed in the following sections.

### A. COMPRESSOR

The three-stage axial compressor facility, presently assembled with a new design of symmetrical blading, was designed to serve as a research tool for a variety of experiments. The facility is shown in Figure 1.

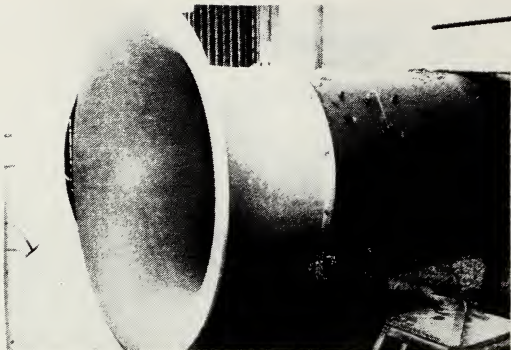
Two different sizes of inlet bellmouths were provided in order to adjust the pressure differential and measure flow rate to the compressor satisfactorily for various stage configurations and operating speeds. In the present work, the larger bellmouth was used (Ref. 2). Views of the bellmouth, with and without a protective mesh screen over the inlet, are shown in Figure 2. As seen in the figure, the airflow enters the compressor from outside the building and flows through a 20-foot long duct containing a throttle device (Ref. 1) to the compressor test section.

The compressor blading is shown in the two parts of Figure 3. The blading is removable and adjustable. For the present experiments, the test section was bladed with one row of inlet guide vanes (IGV), two symmetrical stages (the first stage in Figure 3 was removed), and one row of exit

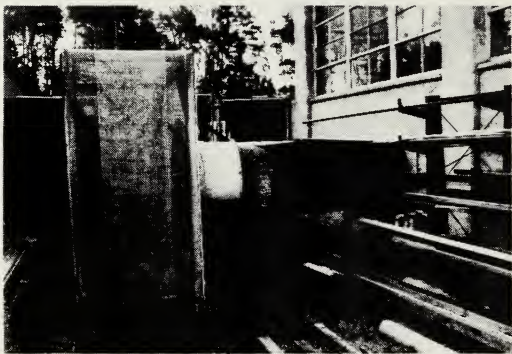


(Dimensions are in inches)

Figure 1. Compressor Test Rig



(a)



(b)

Figure 2. View of the Inlet Bellmouth Without (a) and With (b) a Protective Mesh Screen

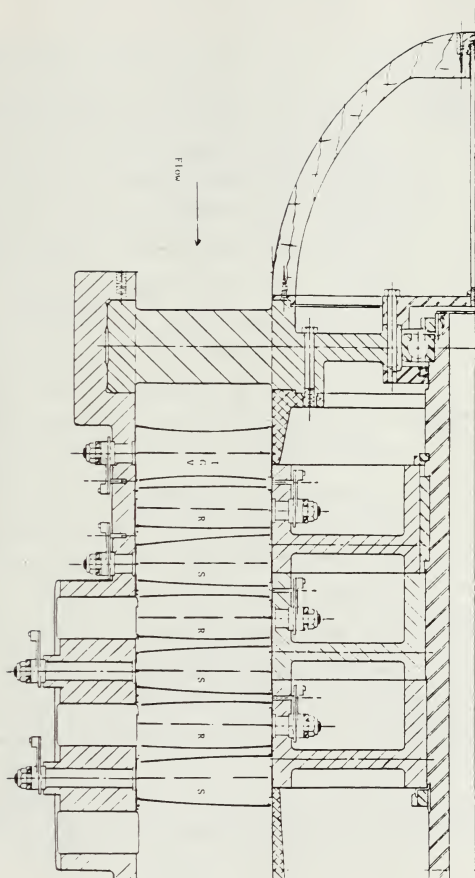


Figure 3. Compressor Blading

(a) Flow Path View



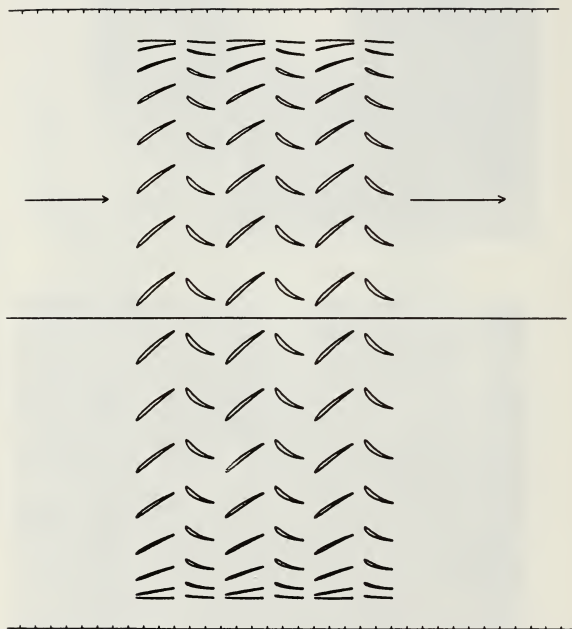


Figure 3. (Continued) Compressor Blading

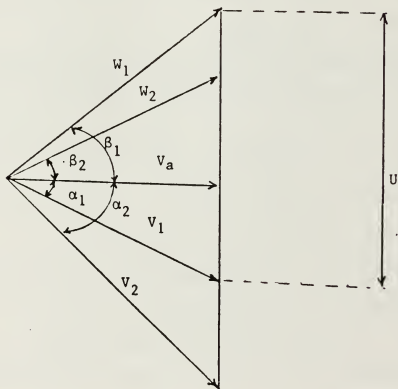
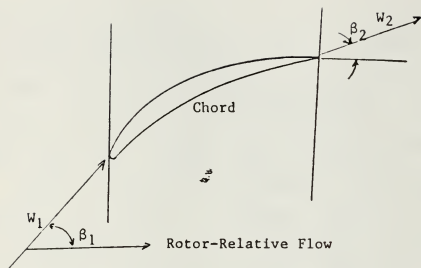
(b) Stage Tip Section

guide vanes (EGV). Each stage consisted of 30 rotor blades and 32 stator blades.

The function of the IGV's is to turn the flow to produce the radial distribution of the flow angle required by the rotor in the symmetric stage. A symmetric stage design is one in which the velocity diagram, shown at one radius in Figure 4, is symmetrical at all radii. (Both the axial velocity component and flow angles vary with radius.) At each radius, the IGV is designed to produce an incidence with respect to the rotor blade equal to the minimum loss incidence for the corresponding two-dimensional compressor cascade (Refs. 3, 4, and 5).

The compressor test rig is shown in Figure 5. The compressor is driven by a 150 HP electric motor coupled by a belt drive to the compressor (Figure 6). The speed of the compressor can be changed nominally from 1600 to 2200 RPM by changing the belt drive pulleys. The low speed drive (1610 RPM) was used in the present experiment.

The throttle, located approximately mid-way between the inlet bellmouth and the compressor face (Fig. 1), contained 10 spaces (8 useable) for inserting different screens and throttle plates. A view of the throttle is shown in Figure 7. The throttle can be changed only by stopping the compressor.



Symmetric Blading Requires  $\alpha_1 = \beta_2$  &  $\alpha_2 = \beta_1$  at All Radial Stations.

Figure 4. Velocity Diagram

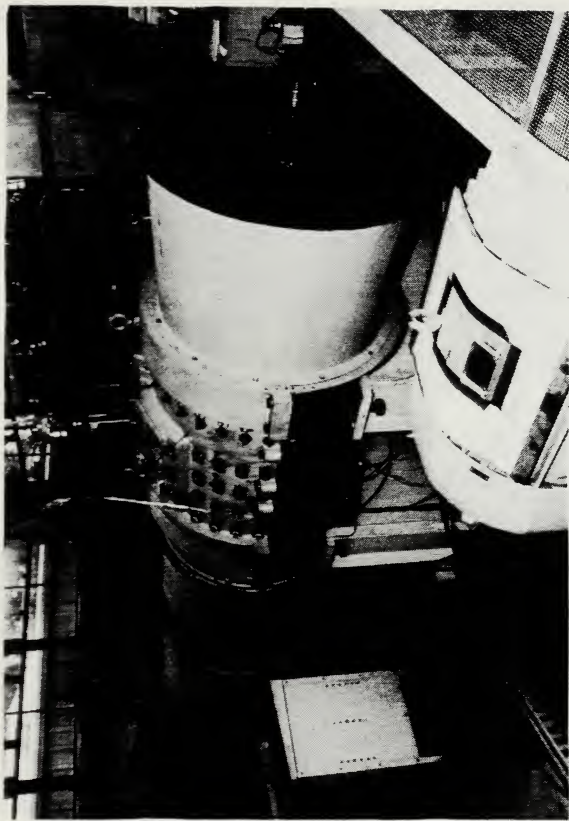


Figure 5. View of the Compressor Test Rig

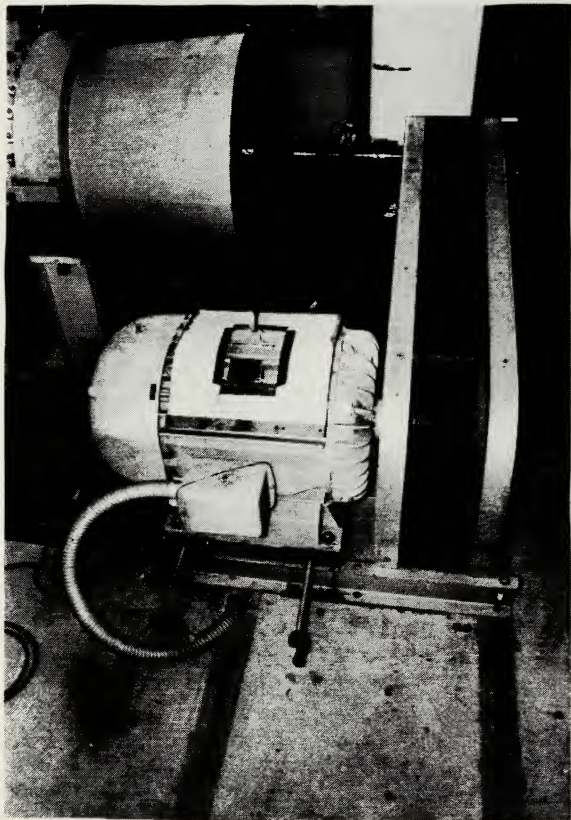


Figure 6. Electric Motor Drive

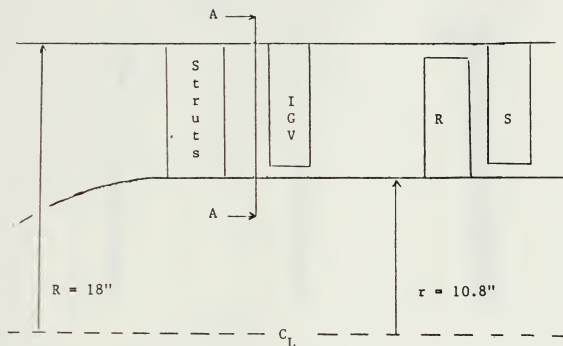


Figure 7. Throttle Showing Removable Elements

All the connections between the inlet bellmouth and the compressor were sealed to eliminate leaks that might effect the experimental results.

### B. INSTRUMENTATION AND DATA COLLECTION

Many ports for probes are provided around and along the compressor case. The arrangement of instrumentation used in the present experiments is shown in Figure 8. Wall static taps and probe survey stations were located 1.0 inches in front of the IGV's at the selected stations around the compressor periphery shown in the figure. Stagnation pressure distributions from tip to hub were measured using a traversing impact probe. A cobra probe was used similarly to measure stagnation pressure and, by prior calibration, static pressure distributions in the same location (Figure 9a and b). In the latter case, pressure ports on each side of the Cobra probe were connected to the U-tube manometer and the probe rotated such that the probe was always facing the airflow. The Kiel probe was installed and held fixed on the centerline of the duct. Pressure distributions in the probe surveys were referenced to corresponding values of total pressure on the centerline and static pressure at the case-wall. The differences between probe total pressure and wall static pressure and between probe total pressure and Kiel probe pressure were recorded manually after carefully adjusting two Meriam micromanometers. The connections to



VIEW A - A

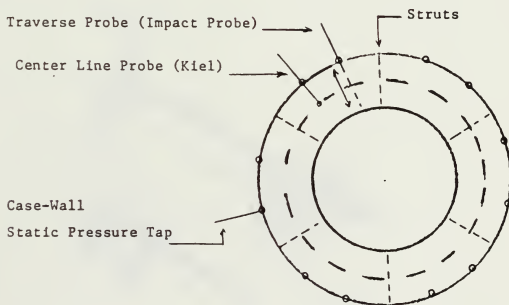
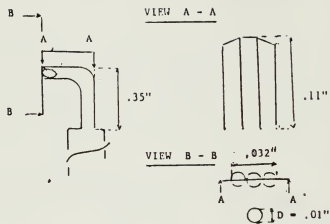
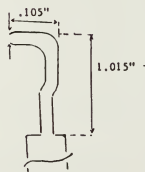


Figure 8. Arrangement of the Instrumentation

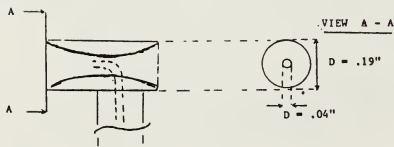




A. Cobra Probe



B. Impact Probe



C. Kiel Probe

Figure 9. Probes  
(a) Probe Tip Geometries

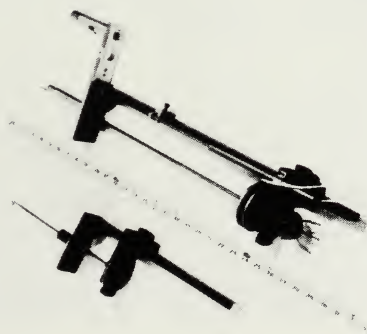
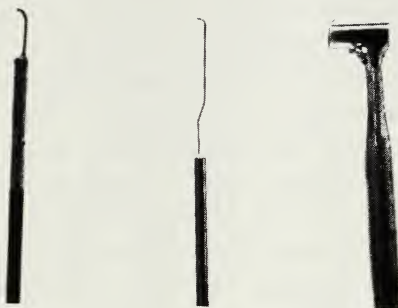


Figure 9. (Continued) Probes  
(b) Views of Probe Tips and Actuators

and a view of the micromanometers are shown in Figure 10.(a) and Figure 10.(b), respectively. The scales of the Meriam manometers were adjusted to zero before each experiment.

Auxiliary instrumentation included a digital thermometer to measure the inlet total temperature and a pulse counter and timing wheel to record the rotational speed of the compressor. The local atmospheric pressure and temperature were measured using a barometer and thermometer respectively, located inside the building. During each test the change in ambient temperature was observed to be negligible and no correction for change in water density in the Meriam watermanometers was required. Air density corrections were not required due to the use of a reference velocity derived from the centerline probe.

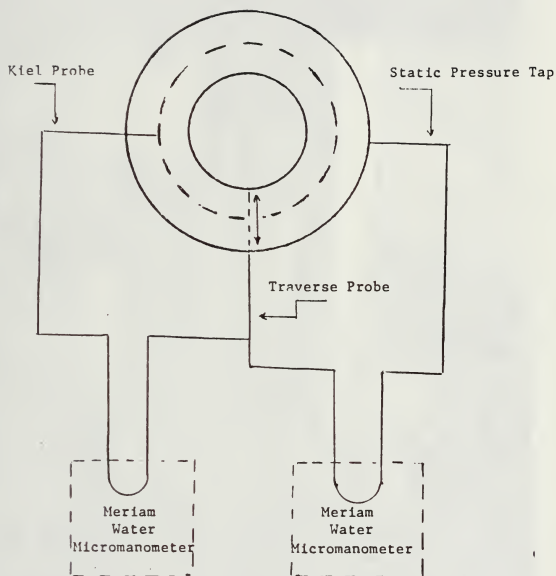


Figure 10. Meriam Water Micromanometers

(a) Connections to the Probes

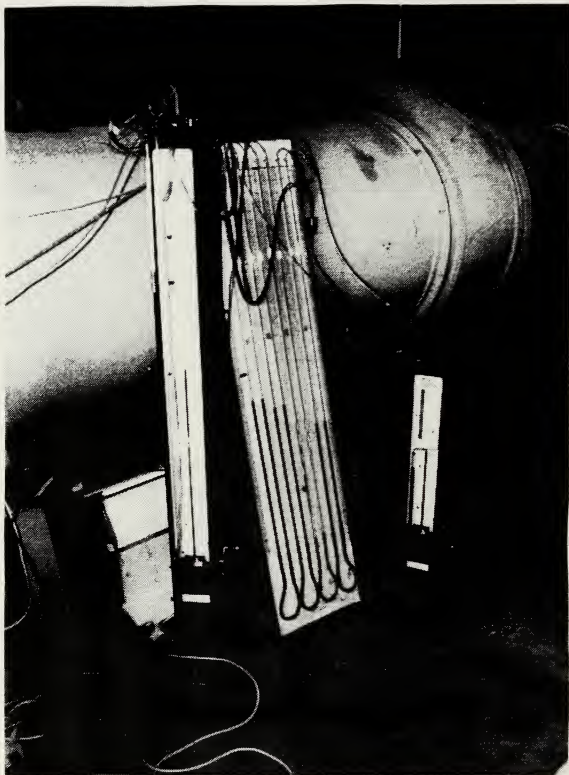


Figure 10. (Continued) Meriam Water Micromanometers  
(b) View of the Instruments

### III. BOUNDARY LAYER CONTROL DEVICE

The boundary layer control device is described in the following section and the design intent, actual design, and construction are discussed.

#### A. DESIGN INTENT

##### 1. Requirements and Approach

Normal boundary layer conditions at the compressor inlet, from earlier experiments with uniform screens, were known to be  $\delta = 1.1$  inches and  $\delta^* = .13$  inches. The boundary layer thickness could be changed by adding a boundary layer control device. Either by sucking air at the case-wall, or by cooling the case-wall, the boundary layer thickness could be reduced. In the planned experiment, it was required to increase the boundary layer thickness ( $\delta^*$ ) by a factor of two and obtain measurements with different values of the tip clearance in the compressor. Thus, it would be possible to obtain data at two values of tip clearance while holding the ratio of boundary to tip clearance [ $\delta^*/t$ ] constant.

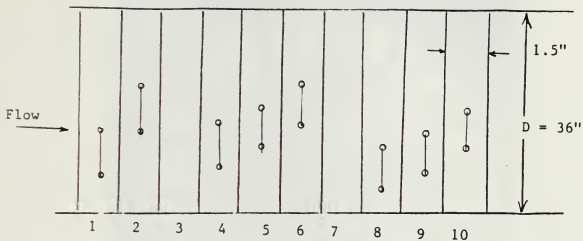
To increase  $\delta^*$  by a factor of two, case-wall roughness elements and graduated screens were both considered, but rejected. The roughness elements could not be removed readily for tests with thin boundary layers. Previous

experience with graded screens suggested that it would be difficult to produce axi-symmetric uniformity with a large graduated screen located so far from the compressor face.

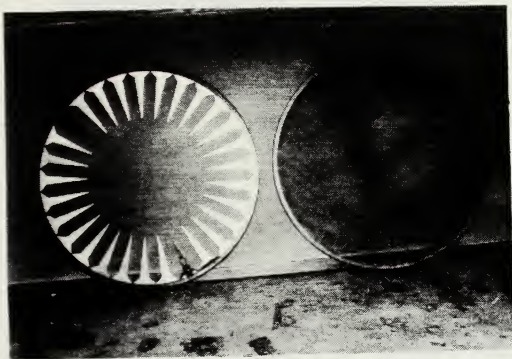
The approach taken was to use "spires" installed in one of the blank throttle elements as shown in Figure 11.

## 2. Design

The system of spires has been used previously to produce thickened boundary layers in rectangular wind tunnels, particularly in experiments which required the careful simulation of the atmospheric boundary layer (Ref. 7). In Reference 7, based on many experiments, the data in Table I were given for a non-dimensional spire geometry that produced a known boundary layer thickness. These data were used in the present design, but were corrected to account for the circular duct configuration and annular flow contraction (Figure 12). The spire geometry and total number of spires were selected using the information in Reference 7 for experiments carried out in a wind tunnel. A 29-element spire configuration was chosen for the circular arrangement to avoid possible resonance due to the wakes from the spires interacting with the 30 blades of the rotor.



a. Element Positions



b. Spire and Plate Elements

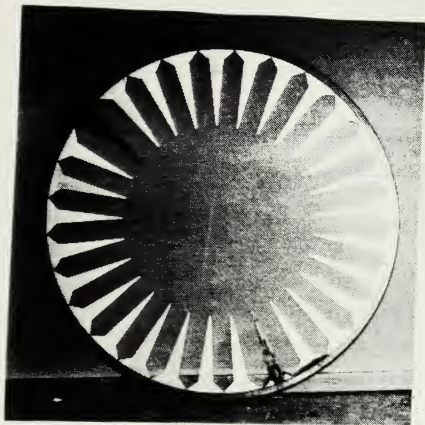
Figure 11. Compressor Throttle Section



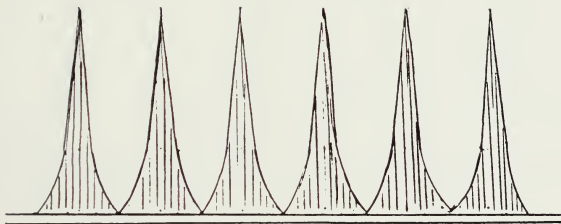
TABLE I.

## DIMENSIONS OF STANDARD HALF-WIDTH SPIRES

<u>HEIGHT</u>	<u>SPIRE WIDTH</u>
0	0.5000
0.0016	0.3750
0.0111	0.3100
0.0167	0.2933
0.0250	0.2733
0.0417	0.2483
0.0833	0.2100
0.1250	0.1850
0.1667	0.1650
0.2500	0.1350
0.3333	0.1117
0.4167	0.0917
0.5000	0.0750
0.5833	0.0600
0.6667	0.0450
0.7500	0.0333
0.8333	0.0217
0.9167	0.0117
1.0000	0.0



a. Circular Arrangement as Built

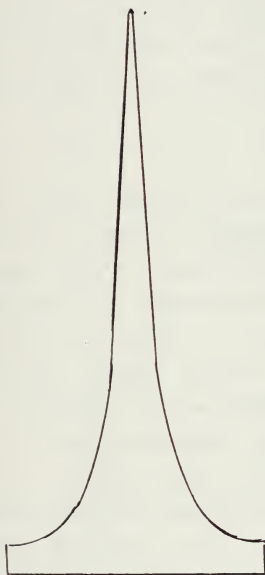


b. Linear Arrangement as Designed

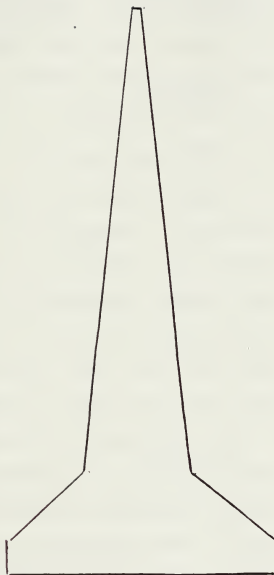
FIGURE 12. Spire Element

## B. CONSTRUCTION

The spire geometry (Figure 13(a)) could not be machined locally, and therefore, the shape was approximated with linear cuts as shown in Figure 13(b). The shape was cut from aluminum alloy, .25 inches thick, and the 29-elements were arranged uniformly in a circular ring. Each spire was attached by three flush, countersunk Phillips-head screws to the rim of the ring. No locking wire was necessary since the screws were prevented from backing out by the adjacent throttle ring installed in the throttle housing, and a screen was positioned downstream of the spires to prevent any possibility of damage to the compressor.



(a) As Designed



(b) As Built

Figure 13. Spire Geometry

#### IV. TEST PROGRAM

The test program consisted of a number of initial, exploratory flow field measurements and then a series of detailed boundary layer surveys to establish quantitatively the effect of the spires on the boundary layer thickness at the compressor face.

##### A. PRELIMINARY TEST

Before conducting detailed flow surveys, tests were conducted to establish an arrangement of screen and spire elements in the throttle which produced a similar average mass rate of through-flow to that produced by a selected combination of screens only (Ref. 8). The desired through-flow condition was one which was well removed from both stall and open throttle boundaries on the compressor map. It was found during this procedure that the position of the spire element in the throttle housing was important. Less stable compressor operation was found when the spire element was the most downstream element. As a result of these tests, the two arrangements summarized in Table II were selected, and the test program summarized in Table III, was carried out.

TABLE II.

## THROTTLE ELEMENT ARRANGEMENTS

THROTTLE ELEMENT LOCATION UPSTREAM	CONFIGURATION (1) SCREEN ONLY	CONFIGURATION (2) SCREEN & SPIRE
1	SCREEN #1	-----
2	-----	SCREEN #5
3	-----	-----
4	-----	-----
5	SCREEN #3	-----
6	-----	SPIRE
7	-----	-----
8	SCREEN #5	-----
9	-----	SCREEN #1
10	-----	-----

TABLE III.		
TEST PROGRAM SUMMARY		
TEST	THROTTLE ELEMENT CONFIGURATION	SURVEYS
1	1	COBRA PROBE & KIEL PROBE
2	1	IMPACT PROBE & KIEL PROBE
3	2	IMPACT PROBE & KIEL PROBE

## B. STATIC PRESSURE DISTRIBUTION MEASUREMENTS

In Test 1, with the throttle elements in configuration 1, a survey was conducted using the cobra probe to establish the radial distribution of static pressure from outer to inner case-wall. The procedure in this experiment was to measure the "indicated" static pressure from the side holes of the cobra probe as it was moved step-by-step from the outer wall to the inner. The relationship of the cobra probe "indicated" static pressure was established using the case-wall static pressure and cobra probe measurements adjacent to the wall. The survey measurements were individually referenced to total pressure from the Kiel probe at the center of the axial line A-A (Figure 8).

The static pressure so obtained is shown in Figure 14. It is seen to decrease linearly from the wall ( $P_{S_W}$ ) to the hub surface.

## C. BOUNDARY LAYER MEASUREMENTS

In Tests 2 and 3, surveys were made using the impact probe from the outer case wall to where the impact pressure became almost constant. Test 2 was with screens only (configuration 1) and test 3 was with the spire element in configuration 2 (Table II). The results are shown plotted in Figure 15 and listed in Table IV and Table V. In Figure 15, the value of the velocity measured on the center line of of the annulus has been used to normalize the profiles.



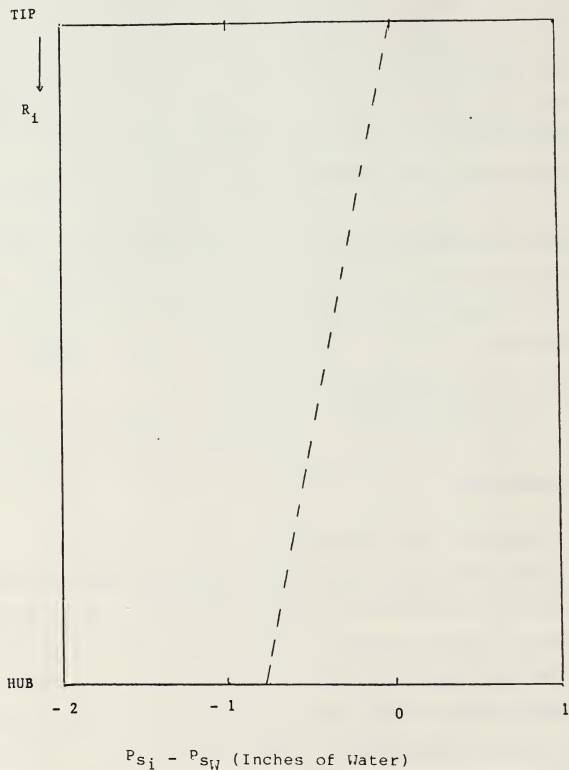


Figure 14. Static Pressure Distribution Ahead of the Inlet Guide Vanes at  $P_{t_{CL}} - P_{sw} = 7.25$  inches of Water

TABLE IV.

PRESSURE DISTRIBUTION DATA FOR CONFIGURATION 1  
 $R_i$  = RADIAL DISPL. INWARDS FROM CASE-WALL,  
 PRESSURES ARE IN INCHES WATER

$R_i$	$P_{t_{CL}} - P_{t_i}$	$P_{t_i} - P_{s_i}$	$P_{t_{CL}} - P_{s_w}$	$V/V_{CL}$	$V/V_\infty$
0.01	7.100	-.060	7.040	-.0902	.0923
0.02	7.092	-.318	7.058	-.0656	.0671
0.1	3.410	3.6466	7.075	.7018	.7179
0.2	2.3195	4.9920	7.197	.8142	.8328
0.3	1.539	5.5672	7.073	.8673	.8872
0.4	1.078	6.0044	7.038	.9030	.9237
0.5	.755	6.3286	7.048	.9264	.9467
0.7	.388	6.7828	7.043	.9594	.9814
0.9	.185	6.9750	7.060	.9717	.9948
1.1	.010	7.1472	7.125	.9792	1.0016
1.5	-.010	7.3271	7.065	.9798	1.0018
2.0	-.0465	7.2882	7.061	.9980	1.0184
2.5	.0	7.3402	7.6500	.9987	1.0187
3.0	.065	7.3518	7.0835	.9991	1.0188
3.4	.071	7.3967	7.1890	.9915	1.0143
3.6	.070	7.4400	7.110	1.0000	1.0299
3.8	.101	7.4702	7.149	1.0002	1.0225
4.2	.009	7.5859	7.1590	1.0068	1.0293
4.5	.006	7.6200	7.126	1.0109	1.0340
5.8	.091	7.7524	7.199	1.0015	1.0337
6.0	.012	7.6776	7.117	1.0153	1.0386

TABLE V.

PRESSURE DISTRIBUTION DATA FOR CONFIGURATION 2  
 $R_i$  = RADIAL DISPL. INWARDS FROM CASE-WALL,  
 PRESSURES ARE IN INCHES WATER

$R_i$	$P_{t_{CL}} - P_{t_i}$	$P_{t_i} - P_{s_i}$	$P_{t_{CL}} - P_{s_w}$	$V/V_{CL}$	$V/V_\infty$
0.01	7.009	-.2179	7.216	-.1710	-.1737
0.02	6.690	.4292	7.1170	.2419	.2456
0.1	3.800	3.2621	7.051	.6698	.6802
0.2	2.634	4.4082	7.0850	.7768	.7887
0.3	2.090	5.0133	7.070	.8292	.8421
0.4	1.848	5.4029	7.207	.8529	.8658
0.5	1.840	5.3526	7.191	.8495	.8627
0.7	1.733	5.5393	7.195	.8614	.8748
0.9	1.497	5.7915	7.189	.8839	.8976
1.1	1.397	5.7872	7.062	.8915	.9053
1.5	1.373	6.1133	7.193	.9078	.9219
2.0	1.000	6.3632	7.141	.9295	.9439
2.5	.915	6.3938	7.123	.9308	.9474
3.0	.484	6.7183	7.136	.9555	.9703
3.4	.032	6.8056	7.157	.9891	.9799
3.6	.156	7.4020	7.178	1.0000	1.0155
3.8	-.117	7.5492	7.264	1.0000	1.0194
4.2	-.227	7.9146	7.221	1.0310	1.0469
4.5	-.911	8.1556	7.098	1.0556	1.0719
5.8	-.411	8.1954	7.143	1.0550	1.0771
6.0	-.337	8.1086	7.105	1.0520	1.0654

## BOUNDARY LAYER

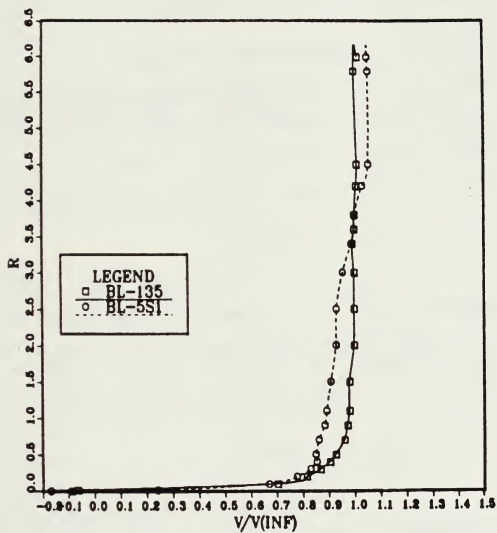


Figure 15. Boundary Layer Profiles With Screens  
(Configuration 1) and Spires (Configuration 2)

## V. ANALYSIS AND DISCUSSION

This section of the report describes the method used to calculate the boundary layer thickness, discusses the results of the measurements in comparison with the design expectation, and summarizes the results.

### A. CALCULATION OF DISPLACEMENT THICKNESS

The displacement thickness obtained for configuration 1 from earlier experiments was .13 and for configuration 2 in the present work was .53 inches. The method was as follows: Bernoulli's equation (Ref. 9) gives, at any radial station,

$$P_{t_i} = P_{s_i} + 1/2 \rho V_i^2 \quad (1)$$

The reference velocity,  $V_\infty$ , based on total pressure at the centerline ( $P_{t_{CL}}$ ) and static pressure at the wall, ( $P_{s_w}$ ) is given by

$$P_{t_{CL}} = P_{s_{CL}} + 1/2 \rho V_\infty^2 \quad (2)$$

Using the results given in Figure 14, which shows that the static pressure dropped linearly to -0.8 inches of water from the tip to the hub at a distance of  $h = 7.2$  inches, at

$$P_{t_{CL}} - P_{s_w} = 7.25 \text{ inches of water,}$$

$$\left( \frac{P_{sW} - P_{si}}{P_{tCL} - P_{sW}} \right) = 0.11 \left( \frac{R_i}{7.2} \right) = 0.0153 R_i \quad (3)$$

Using equations (1), (2) and (3), the ratio of velocity at each point ( $R_i$ ) for configuration (2) is given, in terms of the static pressure distribution for configuration 1, by

$$\frac{V}{V_\infty} = \sqrt{\frac{P_{ti} - P_{sW}}{P_{tCL} - P_{sW}} + 0.0153 R_i} \quad (4)$$

and the centerline velocity by

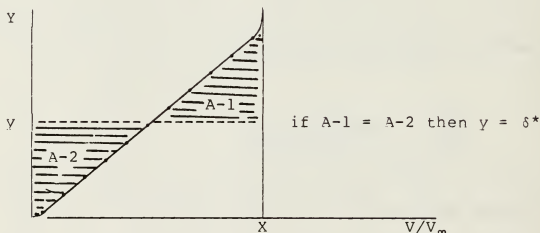
$$\frac{V_{CL}}{V_\infty} = \sqrt{1 + 0.0153 R_i} \quad (5)$$

Using Equation (4) and Equation (5), the ratio of the velocity at each point to the velocity at the centerline is given by

$$\left( \frac{V_i}{V_\infty} \right) / \left( \frac{V_{CL}}{V_\infty} \right) = \frac{V_i}{V_{CL}} \quad (6)$$

From experiment  $P_{t_{CL}} - P_{s_W}$  and  $P_{t_i} - P_{s_i}$  are known at each location from the case-wall to the hub. The boundary layer profiles for configuration 1 and configuration 2 which are shown in Figure 15 were obtained using Equations (4), (5), and (6).

The boundary layer displacement thickness was determined from boundary layer profile data before normalizing to the passage centerline velocity. Referring to the following sketch, the area A-1 and area A-2 were calculated for each displacement ( $y$ ) of the probe from the case-wall using



$$X \cdot y - \int_0^y \left(1 - \frac{V}{V_\infty}\right) dy = A-2 \quad (6)$$

and

$$A_t - \int_0^y \left(1 - \frac{V}{V_\infty}\right) dy = A-1 \quad (7)$$

where  $X$  is the "free-stream" value of  $V/V_\infty$  and  $A_t$  is the total area under the boundary layer profile. The areas

described by equations (7) and (8) were plotted as a function of  $y$  to determine the displacement thickness ( $\delta^*$ ). The results for configuration 1 are shown in Figure 16, with the data listed in Table VI. The results for configuration 2 are shown in Figure 17, with the data listed in Table VII.

## R. COMPARISON WITH DESIGN INTENT

### 1. Boundary Layer Thickness

The effect of the spire element on the boundary layer thickness is clearly to increase  $\delta$  and  $\delta^*$ . Figure 18 illustrates the effect of the spire element on both the boundary layer profile and the boundary layer thickness. The overall thickness was increased from 1.1 to 4.5 inches. The displacement thickness was increased from 0.13 to 0.53 inches. The boundary layer can clearly be controlled by selecting the geometry of the spire, combined with the selection and position of the screens. However, the goal is to produce a doubling of the overall and displacement thicknesses without changing the shape of the profile. Clearly, in the results shown in Figure 18, the overall boundary layer thickness with the spire element exceeds the half-height of the compressor annulus.

We first examine how far the effect of the spire should be expected to extend when the flow from the duct enters the compressor annulus. Referring to Figure 19, the position of the streamline from the tip of the spire, when it



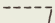
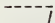
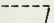
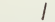
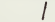

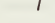

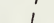





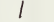
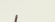


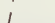
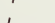
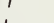
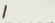


TABLE VI.

INTEGRATED VELOCITY PROFILE PARAMETERS FOR  
CONFIGURATION 1

$R_i$	$\int_0^Y (1-V/V_\infty) dy$	$x \cdot y - \int_0^Y (1-V/V_\infty) dy$	$A_t - \int_0^Y (1-V/V_\infty) dy$
0.0	0.0	0.0	.1473
0.1	.0461	.0539	.1012
0.2	.0703	.1297	.0770
0.3	.0952	.2138	.0611
0.4	.1207	.3023	.0483
0.5	.1473	.3938	.0411
0.7	.1177	.5823	.0296
0.9	.1246	.7754	.0227
1.1	.1295	.8705	.0178
1.5	---	---	---
2.0	/	/	/
2.5	/	/	/
3.0	/	/	/
3.4	/	/	/
3.6	---	---	---
3.6	.1473	3.4527	0.0
3.8	.1473	3.6527	0.0
4.2	.1473	4.0527	0.0
4.5	.1473	4.3577	0.0
5.8	.1473	5.6527	0.0
6.0	.1473	5.8537	0.0

TABLE VII.

INTEGRATED VELOCITY PROFILE PARAMETERS FOR  
CONFIGURATION 2

$R_i$	$\int_0^y (1-V/V_\infty) dy$	$x \cdot y - \int_0^y (1-V/V_\infty) dy$	$A_t - \int_0^y (1-V/V_\infty) dy$
0.0	0.0	0.0	.5716
0.1	.0586	.0470	.5130
0.2	.0901	.1210	.4815
0.3	.1140	.2027	.4576
0.4	.1343	.3880	.4473
0.5	.1537	.4741	.4179
0.7	.1933	.5456	.3783
0.9	.2262	.7238	.3454
1.1	.2580	.9032	.3136
1.5			
2.0			
2.5			
3.0			
3.4			
3.6			
3.8			
4.2			
4.5	.5716	4.1786	0.0
5.8	.5716	5.5501	0.0
6.0	.5716	5.7620	0.0

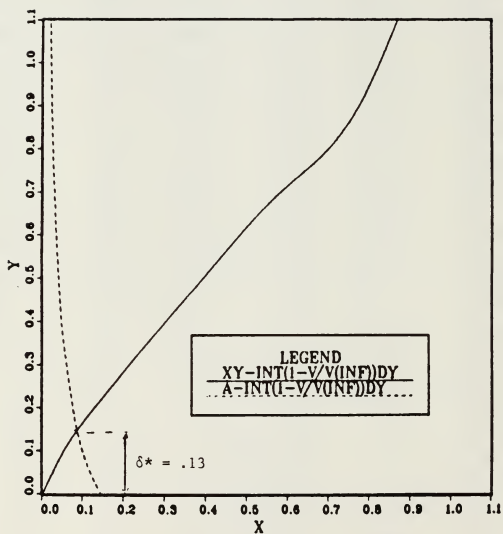


Figure 16. Determination of the Displacement Thickness for Configuration 1

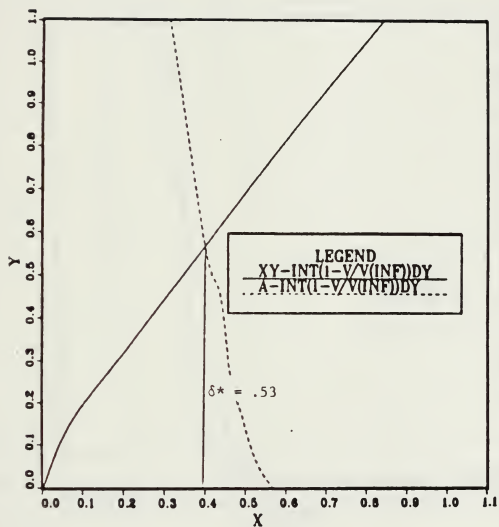


Figure 17. Determination of the Displacement Thickness for Configuration 2

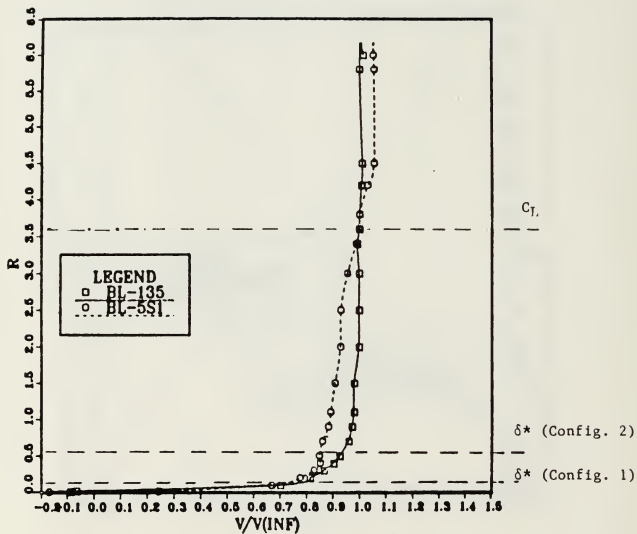


Figure 13. Comparison of Boundary Layers With and Without Spires

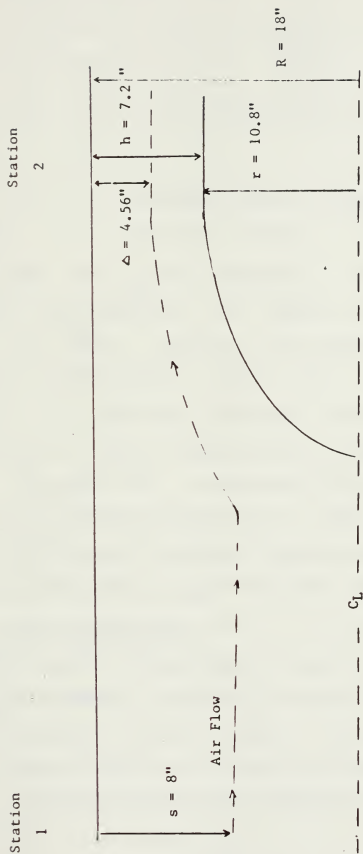


Figure 19. Streamline Location for Uniform Inviscid Flow

approaches the compressor blading can be calculated using the continuity equation,

$$\rho AV = \text{constant} \quad (9)$$

assuming the airflow is uniform and axial at both stations. Then the streamline displacement ( $\Delta$ ) at the compressor face is given by

$$\frac{\rho \pi (R^2 - (R-s)^2)}{\rho \pi R^2} = \frac{\rho \pi (P^2 - (R - \Delta)^2)}{\rho \pi (R^2 - (R - h)^2)} \quad (10)$$

where the notation is defined in Figure 19. The height the spire,  $S = 8$  inches,  $R = 18$  inches, and the annulus height at station 2,  $h = 7.2$  inches. Using these data in equation (10),  $\Delta = 4.56$  inches. The results from the experiment in Figure 18 show that the effect of the circular spire arrangement on the airflow extends to approximately 4.5 inches from the case-wall. In comparison, in the results given in Ref. 7, the effect of a linear arrangement of spires on the boundary layer in the test section of a large wind tunnel, six spire heights downstream, extended to approximately only 0.8 of the spire height from the wall. This factor was applied in arriving at the present spire height. The difference between the present and the wind tunnel results may be due to the significantly different blockage presented by the spires to the pipe flow, or may result from the bluntness of the present shapes.

## 2. Profile Shape

In comparing the two profiles in Figure 18, one significant difference and one noticeable similarity are noted. First, away from the wall, there is a significant departure in the profile shape for configuration 2 from a simple power-law profile. There is seen to be a sharp gradient in the velocity deficit out to the edge of the boundary layer. This is probably the result of the bluntness of the spire shape used in the experiments. The results appear to emphasize the necessity to achieve the very slender, cusped profile shown in Figure 13(a) rather than use the blunt approximation shown in Figure 13(b).

Second, the profile close to the wall seems little affected by the spires. This may be the result of the level of turbulence inherent in the pipe-flow and the pipe-roughness, but suggests that it may be difficult to produce a thicker boundary layer using spires which is also similar in profile shape both near to and far from the wall.

## 3. Other Considerations

The degree of axi-symmetry was examined briefly during the experiments by rotating the spire element in the throttle housing. Some peripheral non-uniformity was detected, however, the data in Figure 18 are believed to be reasonably representative of the average radial behavior. The degree of unsteadiness in the flow, which made it



difficult to obtain stable readings during probe surveys, did not measurably affect the accuracy of the mean velocity profiles.

#### C. ACHIEVING THE REQUIRED CONTROL

The velocity profile shown for configuration 1 in Figure 18 can be characterized as a nearly uniform flow with a well-defined turbulent boundary layer at the case-wall. The velocity profile shown for configuration 2 can be characterized as a very thick, irregular case-wall boundary layer, or alternately described as a wholly distorted velocity profile across more than half the compressor blade height.

Since the purpose of the overall compressor investigation is to examine the effects of tip gap on the compressor flow field and performance characteristics, in a range of tip clearance gap size which is always very much smaller than the blade height, it does not make sense to introduce radial distortions in the flow field which extend over much of the span of the blading. This is not within the scope of the proposed investigation. Any variation in the case-wall boundary layer must be confined to a scale which remains small compared to the blade height or the investigation becomes one of investigating inlet flow distortion.

Thus, if spire elements are to be used, it is very necessary to use the original, sharply cusped spires in order to recover the asymptotic outer boundary layer

profile shape. A reduction in the spire height to 6 or even 5 inches, may be necessary to achieve no more than doubling of the natural boundary layer thickness.

## VI. CONCLUSIONS AND RECOMMENDATIONS

In this study, a ring of spires was designed and shown experimentally to increase the thickness of the case-wall boundary layer at the compressor inlet. While an increase in the overall and displacement thicknesses by a factor of two was intended, a factor close to four was measured. The quantitative differences between results in the present experiment and results obtained using spires to control boundary layers in large rectangular wind tunnels, on which the design of the present arrangement was based, are thought to be understood. First, the slender cusped shape of the spires was approximated in the present case by a blunt, thicker profile which could be machined with straight cuts. Second, the present installation of the spires was within a circular pipe, with a much larger area blockage and higher turbulence levels than were present in the wind tunnel application.

It was found that the ring-element of spires must be installed in the throttle upstream of at least one screen element in order to reduce oscillations in the flow and vibrations in the compressor to acceptable levels.

The following recommendations are made in order to achieve the intended boundary layer control:

1. The originally specified geometrical shape of the spire elements should be machined, without compromise for reasons of expense. The height of the spire should be reduced to 5 or 6 inches.
2. The inlet pipe junctions should be smoothed and all flanged connections should be tightly sealed.

## REFERENCES

1. Waddell, J. L., Evaluation of the Performance and Flow in an Axial Compressor, M.S. Thesis, Naval Postgraduate School, Monterey, California, October 1982.
2. Tobiason, E. A., The Pressure Distribution in a Bellmouth, M.S. Thesis, Naval Postgraduate School, Monterey, California, June 1973.
3. American Institute of Aeronautics and Astronautics, Inc., Aerothermodynamics of Gas Turbine and Rocket Propulsion, Oates, G. C., Editor, 1984.
4. Staff of Lewis Research Center, Aerodynamic Design of Axial-Flow Compressors, NASA SP-36, reproduced by National Technical Information Service, Washington, D.C., 1965.
5. Vavra, M. H., Aerothermodynamics and Flow in Turbomachines, Wiley, New York, 1974.
6. Zucker, R. D., Aerodynamic Analysis, Department of Aeronautics, Naval Postgraduate School, Monterey, California.
7. Standen, N., M., A Spire Array for Engineering Thick Turbulent Shear Layers for Natural Wind Simulation in Wind Tunnels, Ottawa, Canada, 1972.
8. Waddell, J. L., TPL Technical Note 82-01, Multistage Compressor - Flow Losses in Throttle Screens and Plates, February 1982.
9. Zucker, R. D., Fundamental of Gas Dynamics, Matrix Publishers, Inc., 1977
10. Schlichting, H., Boundary-Layer Theory, McGraw-Hill, Inc., 1979.

## BIBLIOGRAPHY

AIAA Education Series, Aerothermodynamics of Aircraft Engine Components, Gordon C. Gates, Editor, 1963

Proceedings of the Symposium on Flow Research on Blading, Flow Research on Blading, Brown, Boveri & Company Limited, Baden, Switzerland, 1969.

Li, W. H. and Lam, S. H., Principles of Fluid Mechanics, Addison Wesley Publishing Company, 1964

Goldstein, R. J., Fluid Mechanics Measurements, Hemisphere Publishing Corporation, 1983.

Moyle, I., Progress Report - Multistage Axial Compressor Program on Tip Clearance Effects, NPS Contractor Report (NPS67-81-01CR), May 1979 - August 1981.

Peacock, R.E., Blade Tip Gap Effects in Turbomachines - A Review, NPS Final Report No NPS67-81-016, October 1980.

McEligot, Capt. D.M., Uniform Inlet Conditions for the NPS Subsonic Cascade Wind Tunnel, Project Report, NPS No. NPS67-81-019PR, January 1981.

Moyle, I. and Zebner, H., Multistage Compressor - Installation of Cast-Epoxy Blades, TPL Technical Note 80-06, October 1980.

Moyle, I. N., Multistage Compressor - Initial Measurement With One Stage of Symmetrical Blading, TPL Technical Note 80-09, October 1980.

Neuhoff, F., Calibration and Application of a Combination Temperature-Pneumatic Probe for Velocity and Rotor Loss Distribution Measurements in a Compressor, NPS Contractor Report No: NPS-67-81-03CR, December 1981.

# INITIAL DISTRIBUTION LIST

	No. of Copies
1. Defense Technical Information Center Cameron Station Alexandria, Virginia 22304-6145	2
2. Superintendent Attn: Library, Code 0142 Naval Postgraduate School Monterey, California 93943-5000	2
3. Chairman Department of Aeronautics and Astronautics, Code 67 Naval Postgraduate School Monterey, California 93943-5000	1
4. Professor R. P. Shreeve, Thesis Advisor Director, Turbooropulsion Laboratory, Code 67SF Department of Aeronautics and Astronautics Naval Postgraduate School Monterey, California 93943-5000	4
5. Naval Air Systems Command (Attn: AIR 931E) Washington, D.C. 20361	1
6. Naval Air Propulsion Center (Attn: Vernon Lubosky) P.O. Box 7176 Trenton, New Jersey 08628	1
7. Professor G. J. Walker Department of Civil and Mechanical Engineering University of Tasmania GPO Box 252C Hobart, Tasmania 7001 Australia	1
8. Dirpers, Mabes TNI-AU Jl Gatot Subroto 72 Jakarta, INDONESIA	1
9. Dirdik, Mabes TNI-AU Jl Gatot Subroto 72 Jakarta, INDONESIA	1
10. Komandan Koharmatau Lanuma Husein Sastanegara Bandung, INDONESIA	2

# INITIAL DISTRIBUTION LIST (CONTINUED)

	No. of Copies
11. Perpustakaan PT. Dirgantara Lanuma Husein Sastaneqara Bandung, INDONESIA	1
12. Muliukur Tarigan Komplek Kartanegara D-5 Singosari-Malang INDONESIA	4
13. Director S. M. A. Negeri Kabanjahe Sumatera Utara INDONESIA	1
14. Wing Pesbang 30 Lanuma Abd. Saleh Malang INDONESIA	1
15. Perpustakaan Lanuma Abd. Saleh Malang INDONESIA	1
16. Wing Pesbang 10 Lanuma Husein Sastranegara Bandung INDONESIA	1
17. Perpustakaan I.T.B. Bandung INDONESIA	1
18. Perpustakaan Universitas U.S.U. Medan, Sumatera Utara INDONESIA	1
19. Perpustakaan Universitas Dirgantara Lanuma Halim P. Jakarta INDONESIA	1
20. Marie Hashimoto Department of Aeronautics and Astronautics, Code 67 Naval Postgraduate School Monterey, California 93943-5000	1









Thesis

T13835 Tarigan

c.1

Development of a boundary layer control device for tip clearance experiments in an axial compressor.

Thesis

T13835 Tarigan

c.1

Development of a boundary layer control device for tip clearance experiments in an axial compressor.



thesT13835

Development of a boundary layer control



3 2768 000 78948 1

DUDLEY KNOX LIBRARY